Fluence rate-dependent intratumor heterogeneity in physiologic and cytotoxic responses to Photofrin photodynamic therapy†

Theresa M. Busch,*[a] Xiaoman Xing,‡[b] Guoqiang Yu,‡[b,e] Arjun Yodh,[a,b] E. Paul Wileyto,[c] Hsing-Wen Wang,[a,b,f] Turgut Durduran,[b,d] Timothy C. Zhu[a] and Ken Kang-Hsin Wang[a]

Received 21st May 2009, Accepted 16th September 2009
First published as an Advance Article on the web 15th October 2009
DOI: 10.1039/b9pp00004f

Photodynamic therapy (PDT) can lead to the creation of heterogeneous, response-limiting hypoxia during illumination, which may be controlled in part through illumination fluence rate. In the present report we consider (1) regional differences in hypoxia, vascular response, and cell kill as a function of tumor depth and (2) the role of fluence rate as a mediator of depth-dependent regional intratumor heterogeneity. Intradermal RIF murine tumors were treated with Photofrin PDT using surface illumination at an irradiance of 75 or 38 mW cm^{-2}. Regional heterogeneity in tumor response was examined through comparison of effects in the surface *vs.* base of tumors, *i.e.* along a plane parallel to the skin surface and perpendicular to the incident illumination. 75 mW cm^{-2} PDT created significantly greater hypoxia in tumor bases relative to their surfaces. Increased hypoxia in the tumor base could not be attributed to regional differences in Photofrin concentration nor effects of fluence rate distribution on photochemical oxygen consumption, but significant depth-dependent heterogeneity in vascular responses and cytotoxic response were detected. At a lower fluence rate of 38 mW cm^{-2}, no detectable regional differences in hypoxia or cytotoxic responses were apparent, and heterogeneity in vascular response was significantly less than that during 75 mW cm^{-2} PDT. This research suggests that the benefits of low-fluence-rate PDT are mediated in part by a reduction in intratumor heterogeneity in hypoxic, vascular and cytotoxic responses.

Introduction

The choice of fluence rate in photodynamic therapy (PDT) can affect treatment outcome.[1–3] PDT is a drug- and light-based approach for treatment of malignant or otherwise abnormal tissues that requires oxygen to produce tissue-damaging reactive oxygen species. Lower fluence rates of illumination lead to lower rates of photochemical oxygen consumption, which in turn permit better maintenance of tumor oxygenation during PDT.[4,5] Studies of several photosensitizers and tumor models have shown an advantage to lower fluence rate. For example, PDT of HT29 human colon adenocarcinoma xenografts with *meta*-tetra(hydroxyphenyl)chlorin (mTHPC) found low fluence rates (5 or 30 mW cm^{-2}) to be associated with longer delays in tumor regrowth than light delivery at higher rates (90 or 160 mW cm^{-2}).[1] Similarly, Photofrin PDT of radiation-induced fibrosarcoma (RIF) murine tumors over a broad range of fluence rates (10–200 mW cm^{-2}) found lower fluence rates to be more efficient.[2] Low fluence rate has also demonstrated advantage in tumors grown in an orthotopic setting. Greater necrosis was found when the fluence rate of interstitial-delivered light was reduced six-fold in aminolevulinic acid (ALA)-induced protoporphyrin IX (PpIX) PDT of orthotopic rat gliomas (BT4C).[3] In PDT of orthotopic rat bladder tumor (NBT-II), both ALA-induced PpIX and benzoporphyrin derivative (BPD) were associated with greater reductions in the surviving fraction of tumor cells for delivery of 30 J cm^{-2} at 30 mW cm^{-2} *vs.* 100 mW cm^{-2}.[6] An important finding of this study was that lower fluence rate benefitted response to both a photosensitizer that is localized to the tumor cells and one that is also within the vasculature at the time of illumination, which suggests that fluence rate can affect both cellular and vascular responses to PDT. Finally, in a clinical study, a significant improvement was reported in the percentage of complete remissions (7 week follow up) of actinic keratosis to ALA-induced PpIX PDT at 30 mW cm^{-2} compared to higher fluence rates of 45, 50 and 75 mW cm^{-2} (effective fluence rates corrected for spectral distribution of the light sources were 9.6 compared to 15, 15, and 22 mW cm^{-2}, respectively).[7]

By slowing the rate of oxygen consumption during PDT, lower fluence rate provides opportunity for oxygen delivery through the tumor blood vessels to keep pace with oxygen consumption by the combination of photochemical and metabolic processes. As a

[a]*Department of Radiation Oncology, School of Medicine, University of Pennsylvania, B13 Anatomy and Chemistry, 3620 Hamilton Walk, Philadelphia, PA 19104-6072, USA. E-mail: buschtm@mail.med.upenn.edu; Fax: +1 215-898-0090; Tel: +1 215-573-3168*
[b]*Department of Physics and Astronomy, School of Arts and Sciences, University of Pennsylvania, Philadelphia, PA 19104, USA*
[c]*Department of Psychiatry, School of Medicine, University of Pennsylvania, Philadelphia, PA 19104, USA*
[d]*Department of Radiology, School of Medicine, University of Pennsylvania, Philadelphia, PA 19104, USA*
[e]*Center for Biomedical Engineering, University of Kentucky, Lexington, KY 40506, USA*
[f]*Institute of Biophotonics, National Yang-Ming University, Taipei, 11221, Taiwan*

† Electronic supplementary information (ESI) available: Fig. S1 (fluence rate as a function of tumor depth); Fig. S2 (EF3 binding level). See DOI: 10.1039/b9pp00004f

‡ These authors contributed equally to this work

result, oxygen depletion relative to distance from a blood vessel should be less severe during low-fluence-rate PDT,[8,9] and indeed *in vivo* data confirm this expectation.[4] Corresponding effects on the distribution of PDT-induced tumor damage have also been reported. For example, low-fluence-rate 2-(1-hexyloxyethyl)-2-devinyl pyropheophorbide-a (HPPH) PDT was associated with widely-distributed apoptosis, while apoptosis was more localized to vascular areas after high-fluence-rate PDT.[8]

In addition to microscopic heterogeneity in oxygen gradients during PDT relative to the tumor vessels, it is also biologically relevant to consider regional heterogeneity in PDT effects along the axis of light delivery. The treatment light is scattered and absorbed by tissue (tumor), leading to measurable gradients in the fluence rate seen by the tissue as a function of distance from the light source. Corresponding fluence rate effects on tumor oxygenation and cytotoxic response may also be present within a tumor. However, the attenuation depth of the 630 nm light typically used in conjunction with Photofrin PDT is reported as ~2–5 mm.[10,11] Thus only limited studies have considered the consequences of light attenuation in murine subcutaneous tumors,[12] which are generally small in size, and corresponding regional data on measures of therapy outcome are needed.

Observations made during an earlier study of microscopic gradients in tumor oxygenation during PDT suggested that significant regional depth-dependent differences in oxygenation may develop during Photofrin PDT of even small (~3 mm in depth) tumors.[4] In this previous report, which examined PDT-induced hypoxia in vascular-adjacent tumor tissue, it appeared that more hypoxia was present in sections from the base of an intradermal tumor compared to sections from the tumor surface (*i.e.* closer to the incident light). Building upon this unexpected finding, in the present report we have specifically considered depth-dependent, regional differences in hypoxia, vascular response, and cell kill during PDT, and we have examined the role of fluence rate as a mediator of depth-dependent regional intratumor heterogeneity.

Methods

Tumor model and PDT

RIF tumors were propagated on the shaved shoulders of 9–11 week old C3H mice (NCI-Frederick, Frederick, MD) by the intradermal injection of 3×10^5 cells. Approximately ~7–9 days later, the tumor and the surrounding area was depilated (Nair), animals received 5 mg kg^{-1} Photofrin (Axcan Pharma Inc., Mont-Saint-Hilaire, Quebec, Canada) *via* tail vein injection, and 24 h later a 1.0–1.1 cm diameter field centered on the tumor was illuminated. At the time of PDT, tumor size was appropriate for the experimental endpoint, *e.g.* tumors $\leq$100 mm^3 in volume were used in tumor response studies, while tumors up to 200 mm^3 were used in studies requiring tumor excision or monitoring. Illumination to a total incident light dose of 135 J cm^{-2} at the indicated fluence rate was performed using a KTP-YAG pumped dye module (Laserscope, San Jose, CA) tuned to produce 630 nm of light. Light was delivered through microlens-tipped fibers (CardioFocus, Norton, MA) and laser output was measured with a power meter (Coherent, Auburn, CA) and adjusted to deliver the prescribed irradiance at the tissue surface. During PDT, mice were anesthetized by inhalation of isoflurane in medical air, delivered through a nosecone (VetEquip anesthesia machine, Pleasanton, CA). Animals studies were reviewed and approved by the University of Pennsylvania Institutional Animal Use and Care Committee.

Immunohistochemistry and analysis

Hypoxia during PDT was labeled with EF3 [(2-(2-nitroimidazol-1*H*-yl)-*N*-(3,3,3-trifluoropropyl)acetamide), as previously described.[4,13] Briefly, EF3 was injected *via* tail vein at 52 mg kg^{-1} within 5 min before PDT began. Immediately upon treatment completion the tumor was excised, coated in Tissue-Tek Oct compound, and frozen. Cryosections (14 μm thickness) were cut, fixed, blocked and stained using a monoclonal antibody to EF3 (ELK5-A8) conjugated to the fluorochrome Cy3 (Amersham Life Sciences, Arlington Heights, IL). In other sections, antibodies were used to label vascular structure (CD31, 1 : 100 for 1 h; BD Pharmingen, San Diego, CA) or vessel maturity (smooth muscle actin, 1 : 100 for 1 h; GeneTex, Irvine, CA). Respective to these primary antibodies, secondary antibodies of Cy5-conjugated mouse anti-rat (1 : 50 for 45 min; Jackson Immunoresearch, West Grove, PA) and FITC-conjugated donkey anti-rabbit (1 : 200 for 1 h; Jackson Immunoresearch) were used. Images were collected by fluorescence microscopy (LabPhot microscope with a 100 W high pressure mercury arc lamp and Photometrics Quantix CCD digital camera).

For the purpose of quantifying EF3 binding, day-to-day variations in the lamp intensity were accounted for based on images of hemacytometer-loaded calibration dye (Cy3 in 1% paraformaldehyde) and a calibrated EF3 tissue value was calculated as the median tissue fluorescence intensity of the EF3 image multiplied by the exposure time (ms) of the standard dye photograph and then divided by the product of the mean fluorescence intensity of the standard dye photograph and the exposure time (ms) for the tissue image. EF3 fluorescence intensity was quantified in Adobe Photoshop for only tissue-containing areas on the section (determined from images photographed after flooding each section with 20 μM of Hoechst 33342). Background fluorescence, quantified as the lowest value on an image, was subtracted from each image. Staining controls included sections receiving no antibody and sections receiving competed EF3 antibody; all controls demonstrated low to negligible staining.

Images of CD31 and smooth muscle actin (SMA) were masked to label stained areas, and then analyzed to determine percentage of the tumor (identified by Hoechst 33342) that is positive for CD31 or SMA. Intervascular spacing was measured as the closest distance between objects that contained contiguous CD31 staining, *i.e.* blood vessels. All analyses were performed using routines in MATLAB (MathWorks, Natick, MA). Controls included slides stained with secondary, but no primary antibody; these controls demonstrated no staining.

Tumor total hemoglobin concentration

Total hemoglobin concentration (THC) was measured by continuous wave broadband diffuse reflectance spectroscopy, as previously described,[14,15] and validated, including the assessment of PDT effects on tumor optical properties.[15] The system consists of a 250 W quartz tungsten halogen lamp (Cuda Fiberoptics,

Jacksonville, FL), a hand-held surface contact fiber-optic probe, a monochromator (Acton Research, Acton, MA) to disperse light from the detection fibers, and a liquid nitrogen cooled CCD camera (Roper Scientific, Trenton, NJ) to image the reflectance spectra from multiple detection fibers simultaneously. The fiber-optic probe consisted of a 400 μm diameter source fiber and ten co-linear 400 μm diameter detection fibers; for this study data collected from source-detector separations of between 1.2 mm and 4 mm were used, depending on the diameter and curvature of the tumor at the position of probe contact to its surface. Because of the linear orientation of the probe, which collected information from only one location, we took measurements at 10–20 locations (acquisition time of 100 ms per measurement) on the tumor in order to collect data representative of the tumor as a whole. The depth of measurement extended from ~0.6 mm to ~2 mm based on the path of detected light between a source-detector pair; this path of detected light is parabolic in shape and extends to a depth that is centered on a distance of approximately one half of the separation between a pair of source and detector fibers. Spectra were collected in the 400–900 nm wavelength range and calibrated based on measurements in a 6 inch diameter integrating sphere (LabSphere Inc., North Sutton, NH). Measurements were collected immediately before and after PDT, but not during light delivery because the handheld probe obstructed the delivery of the light. Data were fit as previously described to determine concentrations of oxyhemoglobin (c_{HbO_2}) and deoxyhemoglobin (c_{Hb}), from which THC was calculated (THC = c_{HbO_2} + c_{Hb}).[14,15]

Tumor blood flow

Tumor blood flow measurements were performed using a previously described and validated diffuse correlation spectroscopy (DCS) instrument,[16] which operates by measuring rapid temporal fluctuations of transmitted light (785 nm) through tissues and then uses the auto-correlation functions associated with these fluctuations to extract information about the motion of tissue scatterers, in this case red blood cells. The DCS probe consists of nine source and four detector fibers, which are arranged in a circular pattern that cover the entire tumor surface, thereby allowing monitoring to take place without a need to move the probe. The probe is focused on the tumor through a camera lens from a distance of 15 cm, which, together with the use of optical filters to block the treatment light from reaching the detectors, allowed monitoring to occur continuously throughout PDT. The detected path of light through tissue between the source and a given detector is parabolic in shape and the probed depth is centered on a distance of approximately one half of the source-detector separation. Accordingly, sources and detectors that are close together collect data from more superficial tumor regions, while sources and detectors that are further apart collect data from predominantly deeper tissue regions. Depth-dependent, intratumor heterogeneity in blood flow during PDT was quantified as the heterogeneity in DCS data collected from different groups of source-detector separations. For this purpose, source-detector separations of 1–1.5 mm, 1.5–2.9 mm, 3.0–3.9 mm, and 4.0–4.4 mm were used for the groupings, based on the availability of source-detector pairs at specific distances and the desire to minimize any contributions from a lateral effect, *i.e.* data collection from only the tumor periphery or its center within any given source-detector grouping. From the above four source-detector groups, data were predominantly collected from four tumor regions, *centered* on tumor depths of ~0.6, ~1.1, ~1.7 and ~2.1 mm. Groups were averaged to describe mean blood flow response. Error bars represent the heterogeneity in response as a function of tumor depth, *i.e.* they indicate the standard deviation in response among the source-detector groups. Data are expressed as a relative change by normalizing to flow values (for the same source-detector pair) in the minute before PDT began. Overall, the maximum depth probed was ~2.2 mm, which is within the ~3 mm depth of the tumors that were measured.

In vivo/*in vitro* clonogenic assay

Tumor-bearing animals were treated with PDT or controls. At the indicated times after treatment, animals were euthanized by CO_2 inhalation, and tumors were excised and divided into three regions along planes perpendicular to the incident light. The central region was collected only to ensure that regions from the tumor base and surface were well-separated, thus this central region was intentionally small and not processed. Regions of tumor surface and base were weighed, minced, and enzymatically digested using a previous described technique[14] in a trypsinizing flask containing 1500 units deoxyribonuclease (Sigma-Aldrich, St. Louis, MO), 1000 units collagenase (Sigma-Aldrich), and 1.5 mg protease (Sigma-Aldrich) dissolved in 6 ml of Hank's Balanced Salt Solution. Cells were plated on 100 mm tissue culture dishes in triplicate, and after ~10 days of incubation (37 °C at 5% CO_2) colonies were fixed, stained (2.5 mg ml^{-1} methylene blue in 30% alcohol), counted, and a plating efficiency was calculated. Due to the necessarily small size of region-specific tumor samples, only the plating efficiency and not the number of clonogenic cells per gram was used as an endpoint because the development of post-PDT edema introduced large variability in the measured weights.

Tumor response assay

Tumor-bearing animals were treated with PDT or used as controls. After PDT- or control-treatment, mice were followed daily to determine the number of subsequent days until tumor volume equalled or exceeded 400 mm^3 (time-to-400 mm^3). Tumor volume was measured in two orthogonal directions and calculated using the formula volume = diameter × width^2 × 3.14/6. A cure was defined as an absence of tumor regrowth at 90 days after PDT.

Light distribution

Light distribution during PDT was measured as a function of tumor depth with a 0.5 mm isotropic detector (CardioFocus, Inc., Marlborough, MA) tracked through an ethanol-sterilized catheter (Best Medical International Inc., Springfield, VA) that was inserted through the tumors at roughly a 45 degree angle relative to the perpendicular (*i.e.* the direction of incident illumination). The catheter entered the tumor midway between the tumor center and its edge, and was extended to the tumor base. Bleeding was minimal and found not to affect the absorption of light by the detector. A motorized control system with a spatial resolution of 0.05 mm was used to drive the detector along the axis of the catheters. A second detector was placed on the tumor surface during treatment. Data were collected, *i.e.* the track length was

scanned, a total of fifteen times over the course of the delivery of 135 J cm^{-2}. The measured data were analyzed using custom programs written in MATLAB. No differences were noted in light distribution as a function of accumulated fluence so data from all fluences were averaged for the purpose of graphical representation.

Tumor photosensitizer concentrations

Tumor-bearing animals were administered Photofrin (5 mg kg^{-1}, i.v.) and 24 h later tumors were excised and divided into three regions, as described above for the clonogenic assay. Photofrin concentration in the tumor regions was measured as previously described.[17]

Power Doppler ultrasound imaging

Power Doppler ultrasound imaging of tumor perfusion was done with a broadband 12–5 MHz transducer using a Philips ATL 5000 (Philips ATL, Bothell, WA) ultrasound scanner. Imaging was done under ketamine/xylazine anesthesia (150/10 mg kg^{-1}) in control animals; mice were kept warm on a heating pad. Over a period of 5 to 10 min ~10 images were acquired of each tumor. On each image, the tumor was identified, and regions of interest were defined that included the top and bottom thirds of the tumor. Within the regions of interest, the color-weighted fractional area was calculated as a measure of tumor perfusion, as we have previously described.[16] Briefly, the color-weighted fractional area is the product of a mean color level (related to red blood cell flux) and the fractional area covered by the colored pixels (area of perfusion), and thereby provides a measure that is proportional to the blood volume.

Statistics

PDT-induced changes in total hemoglobin concentration (within the same tumor) and regional differences in EF3 binding, plating efficiencies and tumor perfusion (power Doppler ultrasound) were assessed by signed-rank tests. Comparisons across tumors, *e.g.* between control and PDT-treated animals in EF3 and clonogenic studies, were performed by the Wilcoxon test. Immunohistochemical analysis of tumor vessels involved averaging results from multiple sections (when available) collected from either the tumor surface or base, followed by assessment *via* a *t*-test. These tests were performed in JMP 7 (SAS, Cary, NC). Summary characteristics describing blood-flow during PDT, including minimum, maximum, and coefficient of variation, were generated from the time-series. Differences in summary characteristics were tested using *t*-tests, in a linear-regression framework, using bootstrap estimates of standard error. Time series of tumor blood flow were analyzed using Stata (Stata Corporation, College Station, TX). For all tests, $p < 0.05$ was considered significant.

Results

PDT creates regional intratumor heterogeneity in hypoxia

These investigations of fluence rate effect on intratumor heterogeneity in physiologic response evolved from our observation that PDT at a moderate fluence rate of 75 mW cm^{-2} led to not only increases in hypoxia marker (EF3) binding, but also to regional variability in PDT-created hypoxia between sections collected from different tumor depths.[4] Sections of intradermal tumors were cut parallel to the skin surface, *i.e.* perpendicular to the incident illumination, from regions at the tumor base (within 600 μm above the deepest edge) and the tumor surface (within 600 μm below the subcutis). Fig. 1 summarizes the results, showing that compared to sections from control animals, Photofrin PDT at 75 mW cm^{-2} led to significant increases in EF3 binding. Furthermore, regional heterogeneity in hypoxia development during PDT is demonstrated by a greater PDT-induced increase in hypoxia in sections from the tumor base. Median EF3 binding was 2-fold greater in the base *vs.* surfaces of tumors treated with 75 mW cm^{-2} PDT (see also Fig. 5A). Because EF3 incubation took place only during the illumination period for PDT, hypoxia labeling is indicative of tumor oxygen status during PDT when oxygen is required for type II photochemistry and production of reactive oxygen species.

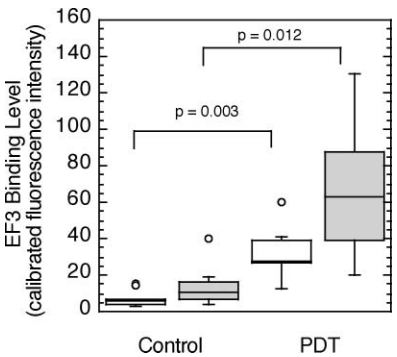

Fig. 1 EF3 labeling of hypoxia during 75 mW cm^{-2} PDT (135 J cm^{-2}). PDT-treated animals ($n = 7$) received Photofrin, EF3 and illumination; controls ($n = 10$) received only EF3 or EF3 and illumination, but no Photofrin. Tumor sections cut parallel to the overlying skin of intradermal tumors were divided into those from within 600 μm below the subcutis (open boxes) or within 600 μm above the tumor base (shaded boxes). Box plots indicate the data range (error bars) with outliers shown as individual points (circles); upper and lower quartiles are indicated by the box with an additional horizontal line to label the median.

In order to consider possible causes for regional inhomogeneity in hypoxia development during PDT, contributions from regional differences in photosensitizer uptake and light distribution were examined. Fig. 2A demonstrates that no difference in Photofrin concentration was found between the base and surface of tumors; median (±SE) photosensitizer concentration was 7.12 ± 1.66 ng mg^{-1} and 6.08 ± 0.60 ng mg^{-1}, respectively. The light distribution within the tumor varied as expected, namely the incident fluence rate increased in more superficial tumor regions and then decreased with depth. During 75 mW cm^{-2} PDT, fluence rate was on average (±SD) 166 ± 20 mW cm^{-2} on the skin surface and 127 ± 3 mW cm^{-2} just under the skin (estimated tumor surface). Fluence rate at the tumor surface was on average 1.5 ± 0.1 times higher than that in the base (depth of ~3 mm) of the same tumor (Fig. 2B). Accordingly, at the tumor base (average fluence rate 93 mW cm^{-2}) one could expect to find less photochemical-induced oxygen consumption than at the tumor surface (average fluence rate 127 mW cm^{-2}), which fails to explain the increase in hypoxia in this (base) region.

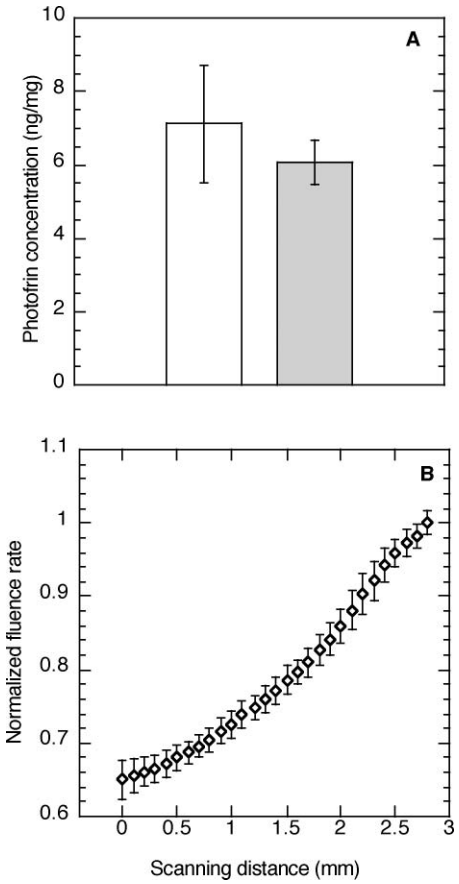

Fig. 2 Depth-dependent regional heterogeneity in tumor Photofrin concentration and light distribution during PDT. Tumor Photofrin concentration (A) was measured by spectrofluorometric assay in regions collected from the tumor surface (open box) or base (shaded box) at 24 h after i.v. administration of 5 mg per kg Photofrin ($n = 5$ animals); the plot shows median ± SE (error bars). Representative plot of light distribution (B) during Photofrin PDT (75 mW cm^{-2}, 135 J cm^{-2}); an isotropic detector was tracked from the base (0 mm) to the surface (3 mm) of a tumor at 45° relative to the incident illumination. Data are normalized to the fluence rate at the tumor surface with points and error bars indicating the mean ± standard deviation of 15 motorized scans throughout the tumor depth over the course of illumination.

In addition to photochemical oxygen consumption, PDT-induced decreases in tumor blood flow could also contribute to hypoxia development during illumination. In order to assess whether blood volume changed over the course of PDT, the PDT effect on total hemoglobin concentration (THC) was measured in each tumor (Fig. 3). Most tumors exhibited a PDT-induced decrease in THC, making the mean change in THC during PDT a value of −12 μM ($p = 0.002$). This suggests that hypoxia during PDT may at least in part be a consequence of decreased tumor perfusion.

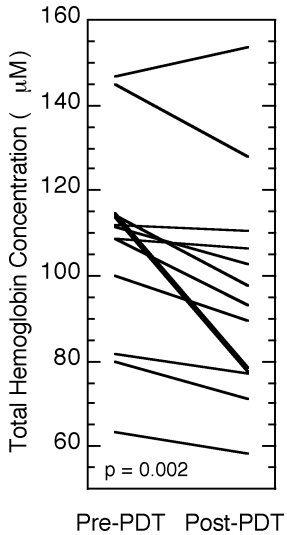

Fig. 3 PDT effect on tumor total hemoglobin concentration (THC). Diffuse reflectance spectroscopy (DRS) was used to measure tumor-averaged THC immediately before and after PDT (Photofrin, 75 mW cm^{-2}, 135 J cm^{-2}). Plots depict the change in individual tumors.

Vascular response is regionally heterogeneous during PDT

In order to more carefully consider spatial heterogeneity in vascular response during PDT, diffuse correlation spectroscopy (DCS) was applied to assess tumor blood flow. Fig. 4A shows a representative trace of relative blood flow during 75 mW cm^{-2} PDT, revealing a strong but temporary PDT-induced increase in blood flow at the initiation of illumination. Curves plot the

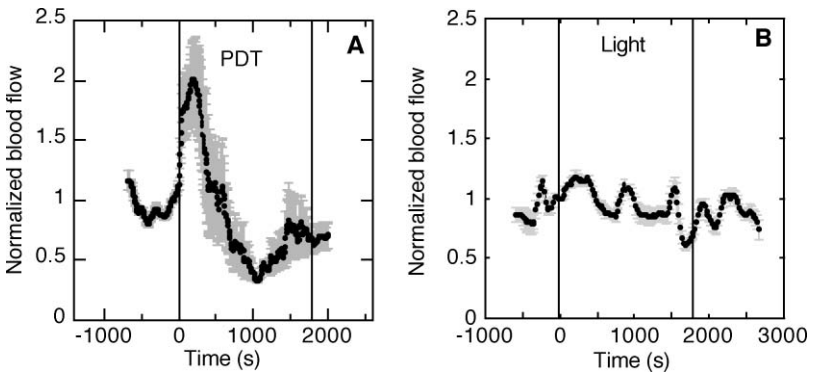

Fig. 4 Representative plots of normalized change in tumor blood flow during Photofrin PDT (A) or control light (B) treatment. The period of illumination (75 mW cm^{-2}, 135 J cm^{-2}) is indicated by vertical lines. Data points indicate average response ± standard deviation (error bars) as a function of source–detector spacing, which provides information on heterogeneity in vascular response over tumor depth.

mean change in blood flow with error bars that represent the standard deviation in vascular response as a function of the separation distance between source-detector pairs in the DCS probe. Source-detector separation is a determinant of the depth of tissue probed, so by organizing the data in this manner, the error bars are representative of heterogeneity in vascular response that is primarily a consequence of tumor depth.

In contrast to vascular response during PDT, control animals exposed to only light (Fig. 4B) demonstrate little intratumor heterogeneity (error bars) in blood flow. In some animals blood flow did fluctuate over time, even under control conditions, but PDT consistently produced a prominent change in blood flow regardless of any fluctuations prior to illumination. Among PDT-treated tumors, the average (±SE) of normalized blood flow ranged from a minimum of 0.5 ± 0.07 to a maximum of 1.7 ± 0.1, while in the light-only controls this range was only 0.9 ± 0.04 to 1.3 ± 0.05 ($p = 1.9 \times 10^{-9}$ and 0.007 for differences between PDT and control groups in the minimum and maximum, respectively). The treatment-averaged coefficient of variation in normalized blood flow was 15 ± 3% in PDT-treated tumors *vs.* 5 ± 0.4% in light controls ($p = 0.0001$).

Low fluence rate reduces regional heterogeneity in physiologic response during PDT

Given findings that a fluence rate of 75 mW cm^{-2} led to significant PDT-created hypoxia and regional intratumor heterogeneity in hypoxia and blood flow, we next examined whether a lower fluence rate previously documented to reduce hypoxia during PDT[4] would also affect intratumor heterogeneity in PDT responses. First, light distribution during 38 mW cm^{-2} was measured and, as in the case of 75 mW cm^{-2} PDT, found to be 1.6 ± 0.4 (mean ± SD) higher at the tumor surface (average fluence rate 55 mW cm^{-2}) than base (average fluence rate 37 mW cm^{-2}). Notably, although the relative intratumor distribution of light was the same in 38 and 75 mW cm^{-2} PDT-treated tumors, the absolute range of fluence rates within tumors that received 38 mW cm^{-2} PDT was necessarily smaller than the range in tumors treated with 75 mW cm^{-2}. Fig. S1† depicts this result for representative tumors during their treatment with either 38 or 75 mW cm^{-2} PDT (range = ~30–45 mW cm^{-2} at 38 mW cm^{-2} and ~70–110 mW cm^{-2} at 75 mW cm^{-2} PDT).

Regional heterogeneity in PDT-induced hypoxia was determined as the ratio of EF3 binding in sections from a tumor's base *vs.* surface (Fig. 5A). As mentioned earlier, during 75 mW cm^{-2} PDT there was 2.2 ± 0.6 (median ± SE) times more hypoxia at the tumors' base than at the surface, which was significantly greater ($p = 0.04$) than a value of one (indicative of no difference). A similar regional differential was not found during 38 mW cm^{-2} PDT; for this condition the ratio of EF3 binding in the tumor base *vs.* surface was 1.1 ± 0.3. Importantly, these results do not indicate that 38 mW cm^{-2} PDT did not create any tumor hypoxia, but rather they emphasize that the 38 mW cm^{-2} fluence rate did not lead to the significant regional heterogeneity in hypoxia found at 75 mW cm^{-2}. 38 mW cm^{-2} PDT did lead to an increase in hypoxia compared to controls (Fig. S2†), but the levels of hypoxia were less than that found at the base of 75 mW cm^{-2}-treated tumors (compare to Fig. 1). Mean (time-corrected) EF3 binding levels at the surface and base of 38 mW cm^{-2}-treated tumors were similar to each other (20 and 24 units, respectively) and to that found at the surface of 75 mW cm^{-2}-treated tumors (33 units), but less than that found at the base of 75 mW cm^{-2}-treated tumors (66 units).

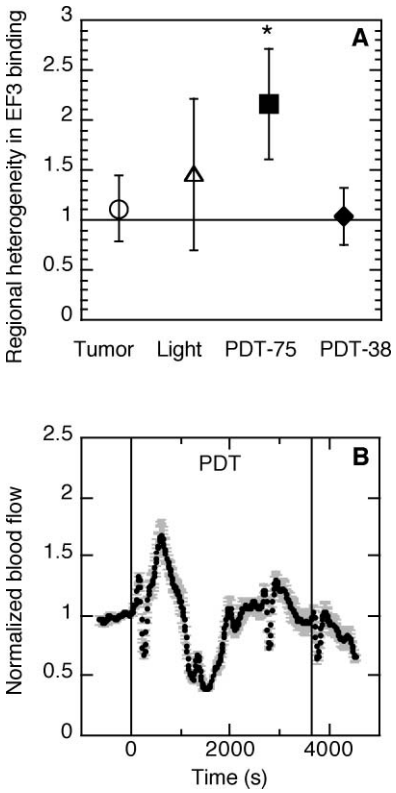

Fig. 5 Depth-dependent regional heterogeneity in tumor hypoxia and blood flow during PDT. Heterogeneity in PDT-created hypoxia (A) is quantified as the ratio of EF3 binding in the base *vs.* surface of a tumor; data are the average ± SD (error bars) of tumors ($n = 6$–8 per group) treated as unilluminated or light-only controls (open symbols), or with PDT (135 J cm^{-2}) at 75 or 38 mW cm^{-2} (closed symbols; * indicates $p < 0.5$ for an increase in hypoxia by one-sided signed rank test). A representative plot (B) of tumor blood flow during 38 mW cm^{-2} PDT (135 J cm^{-2}; indicated by vertical lines). Data points indicate average response ± standard deviation (error bars) as a function of source–detector spacing, which provides information on heterogeneity in vascular response over tumor depth. For comparison, blood flow during 75 mW cm^{-2} PDT is shown in Fig. 4.

Vascular response during 38 mW cm^{-2} was measured by DCS, and a representative plot is shown in Fig. 5B. PDT induced an initial increase in blood flow that was similar to that found with 75 mW cm^{-2} PDT, and maximum (mean ± SE) normalized flow was indistinguishable between 38 mW cm^{-2} and 75 mW cm^{-2} PDT (1.8 ± 0.2 *vs.* 1.7 ± 0.1, respectively). However, blood flow during 38 mW cm^{-2} PDT was distinguished by the facts that a lower minimum was reached (0.3 ± 0.03 *vs.* 0.5 ± 0.07 at 75 mW cm^{-2}, $p = 0.03$), and a return to the pre-treatment level during the latter part of 38 mW cm^{-2} PDT permitted flow maintenance at the 0.75–1.00 level over 26 ± 5% of the total dose at 38 mW cm^{-2} compared to only 13 ± 2% of the total dose at 75 mW cm^{-2} ($p = 0.02$). Reductions in regional intratumor heterogeneity in vascular response during 38 mW cm^{-2} PDT are readily visible as smaller error bars on the graph, and can be quantified by a significant decrease in the coefficient of variation (9 ± 1% *vs.* 15 ± 3% at 75 mW cm^{-2}, $p = 0.0001$).

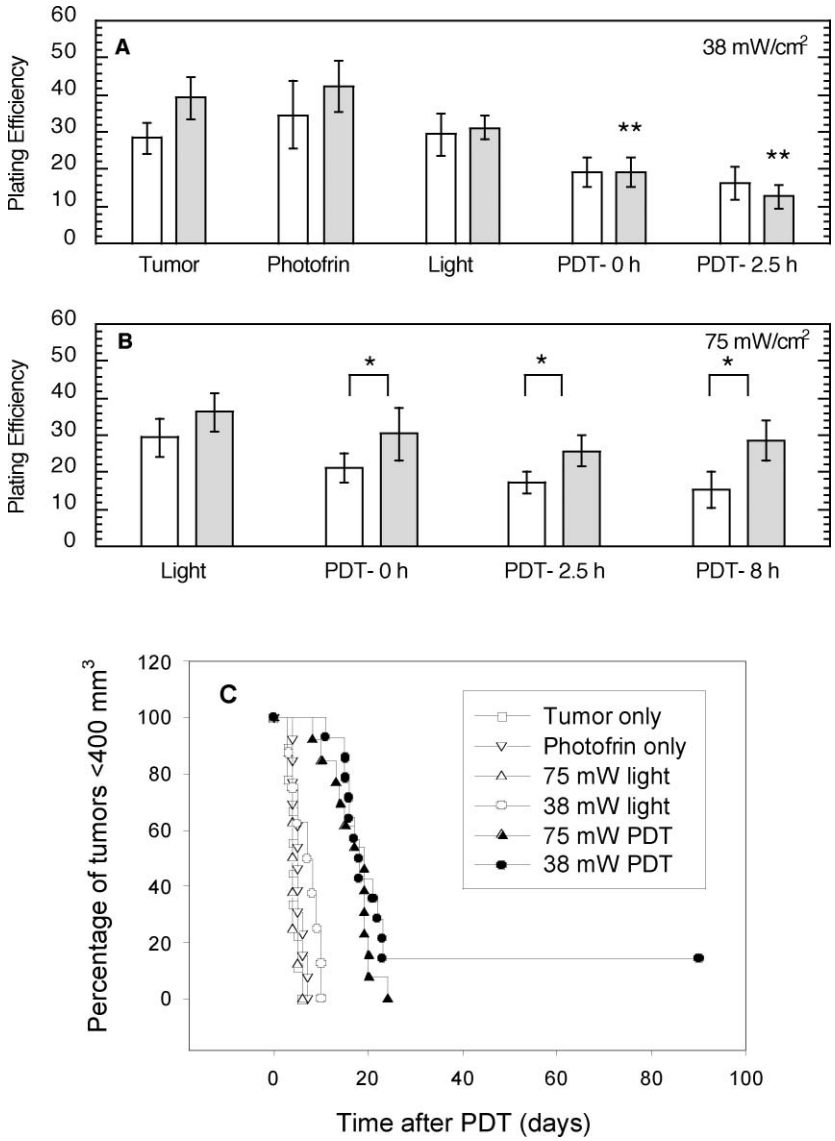

Fig. 6 Short and long term cytotoxic response to 38 mW cm^{-2} *vs.* 75 mW cm^{-2} PDT (135 J cm^{-2}). *In vivo/in vitro* clonogenic assays were used to assess the plating efficiencies of cells isolated from the surface (open bars) *vs.* base (shaded bars) of 38 mW cm^{-2} (A) and 75 mW cm^{-2} (B) treated tumors at the indicated times after PDT ($n = 5$–7). Controls receiving neither light nor Photofrin or only Photofrin are indicated on plot A, while light controls specific to each fluence rate are shown on their respective plots. * indicates $p < 0.05$ for comparison between tumor regions (surface *vs.* deep); ** indicates $p < 0.05$ for comparison to controls (tumor alone). Long-term tumor response (C) is summarized by Kaplan Meier curves with an endpoint of a tumor volume of ≥400 mm^2. Tumor cures, *i.e.* no tumor recurrence within 90 days after PDT, are indicated as hanging points.

Low fluence rate reduces regional heterogeneity in cytotoxic response to PDT

To determine if heterogeneity in tumor oxygenation and blood flow during PDT led to heterogeneity in PDT-induced cytotoxicity the *in vivo/in vitro* clonogenic assay was employed to compare the plating efficiency, *i.e.* the percentage of cells giving rise to colonies, of tumor regions (surface *vs.* deep) collected at various timepoints after 75 mW cm^{-2} or 38 mW cm^{-2} PDT. Only the lower fluence rate led to significant decreases in plating efficiency after PDT (in the tumor base). Furthermore, no difference in the plating efficiency of surface *vs.* deep tumor regions was detected after 38 mW cm^{-2} PDT (Fig. 6A). Interestingly, since controls trended (nonsignificantly) toward a better plating efficiency in cells isolated from the tumor base, PDT at 38 mW cm^{-2} eliminated any differential between the tumor regions. In contrast, PDT at 75 mW cm^{-2} accentuated regional differences in plating efficiencies because significantly less cell death was found in the deep tumor regions, even at times as long as 8 h after PDT (Fig. 6B). These data also demonstrate that the plating efficiency of the surface and base of 38 mW cm^{-2}-treated tumors, *i.e.* 19% for both levels at a time immediately after PDT, was similar to the plating efficiency of the surface of 75 mW cm^{-2}-treated tumors (21%). Compared to these three groups, however, greater protection was found at the base of 75 mW cm^{-2}-treated tumors, which had a plating efficiency of 30% immediately after PDT.

A tumor response assay was used to evaluate overall tumor response to 38 mW cm^{-2} and 75 mW cm^{-2} PDT (Fig. 6C). These

long-term studies found only the low fluence rate capable of producing any cures. All tumors treat with 75 mW cm^{-2} PDT regrew to 400 mm^3 within ~25 days after PDT.

Depth-dependence of tumor vascular microenvironment

The above data document that an average spread of fluence rates from 127 mW cm^{-2} at the surface to 93 mW cm^{-2} at the base of 75 mW cm^{-2}-treated tumors leads to greater heterogeneity in hypoxic, vascular, and cytotoxic responses than does the smaller average spread from 55 mW cm^{-2} at the surface to 37 mW cm^{-2} at the base of 38 mW cm^{-2}-treated tumors. In addition to this conclusion, these data also show that tumor surfaces exposed to 127 mW cm^{-2} (at 75 mW cm^{-2}) *vs.* 55 mW cm^{-2} (at 38 mW cm^{-2}), demonstrated similar hypoxia and cytotoxic responses to PDT, while tumor bases exposed to lower fluence rates over the smaller range of 93 mW cm^{-2} (at 75 mW cm^{-2}) *vs.* 37 mW cm^{-2} (at 38 mW cm^{-2}) demonstrated different hypoxic and cytotoxic responses to PDT. These data suggested to us that an inherent difference exists between the tumor base and surface that makes the base more sensitive to fluence rate effects.

The presence of differences between the microenvironments within a tumor's base and surface were examined to assess this as a possible cause of the increased sensitivity of the base to fluence rate effects in PDT. Studies were focused on the vascular microenvironment because from our above data the response of tumor blood vessels to PDT appears to dominate heterogeneity in fluence rate effects. Power Doppler ultrasound found tumor bases to be better perfused than their corresponding surfaces (Fig. 7A). Using immunohistochemistry, the fraction of tumor positive for CD31, a marker of blood vessel structure, was quantified and found to be the same in sections collected from the tumor base *vs.* surface (Fig. 7B), however the CD31-identified blood vessels were significantly closer together in the tumor base (Fig. 7C). Furthermore, in the base a greater fraction of the tumor stained positive for smooth muscle actin, a marker of vessel maturity (Fig. 7D). Together these data suggest the presence of a more functional network of blood vessels at the base *vs.* surface of these tumors, which could in part explain the increased sensitivity to fluence rate within the tumor base.

Discussion

Low fluence rate is known to benefit PDT response because of its oxygen conserving effects. The present data support the conclusion that the benefit of low fluence rate Photofrin PDT is mediated in part through reductions in regional depth-dependent heterogeneity in PDT responses, even over small distances potentially less than the penetration depth of 630 nm light. PDT at 75 mW cm^{-2} led to significant depth-dependent heterogeneity in PDT-created hypoxia, which was consistent with findings of

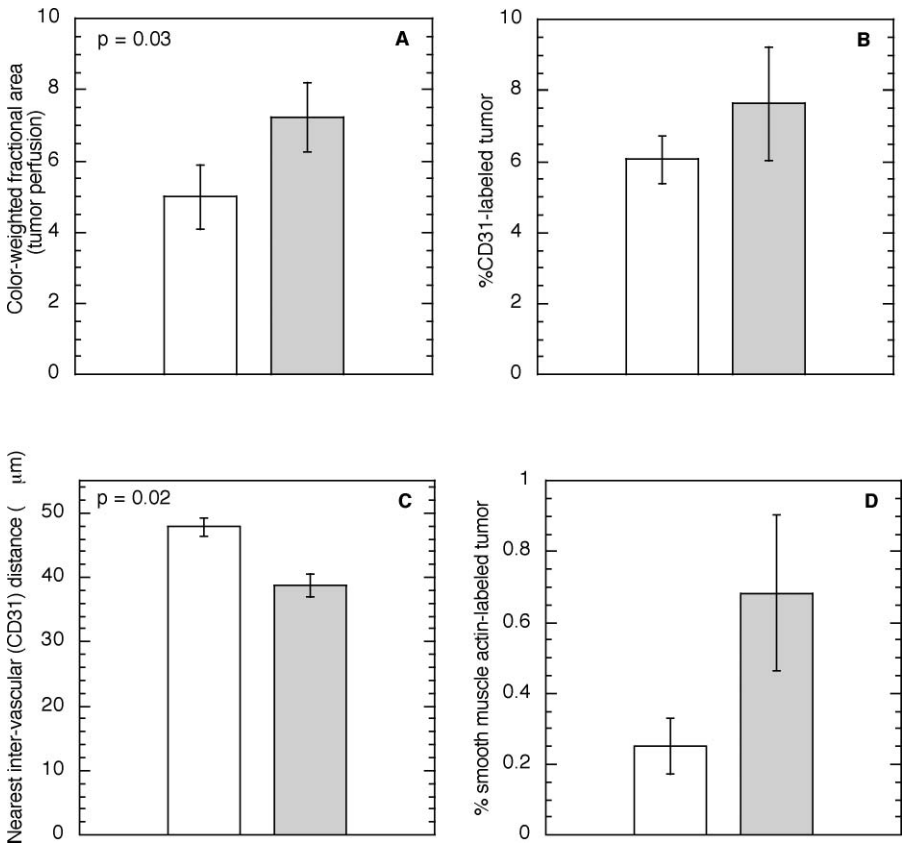

Fig. 7 Perfusion (A), vascular area (B), inter-vascular spacing (C), and mature vascular area (D) in the surface (open bars) *vs.* base (shaded bars) of RIF tumors. Perfusion measured by power Doppler ultrasound as the color-weighted fractional area (see Methods) in 20 control tumors. Vascular areas and spacing measured by immunohistochemical assessment of CD31 (labels endothelial cells) and smooth muscle actin (labels mature vasculature) staining in tumor sections; analysis incorporates 6–12 sections collected from the different tumor levels in 3 mice.

heterogeneity in vascular responses, making it likely that PDT effects on tumor blood flow were the predominant cause of regional hypoxia heterogeneity during 75 mW cm^{-2} PDT. These physiologic heterogeneities did impact outcome: clonogenic assays found significantly greater tumor cell survival in tumor bases, thus suggesting that hypoxia in the tumor base during PDT had a protective effect. Importantly, a lower fluence rate was successful in reducing depth-dependent regional heterogeneities in physiologic and cytotoxic response.

Findings of less intratumor heterogeneity in PDT response to low fluence rate are novel, but also consistent with expectations based on knowledge that the absolute range of fluence rates to which a tumor is exposed will be smaller as fluence rate is lowered. For example, in our studies, PDT at 75 mW cm^{-2} was associated with an average fluence rate of 127 and 93 mW cm^{-2} in the tumor surface and base, respectively, while PDT at 38 mW cm^{-2} was associated with an average fluence rate of 55 and 37 mW cm^{-2} in the tumor surface and base, respectively. Thus, the tumors treated with high fluence rate experienced a ~2-fold greater range of fluence rates. Fluence rate is known to have an effect on the severity and time course of vascular damage after PDT,[18,19] so it is reasonable to expect that intratumor heterogeneity in fluence rate distribution would lead to intratumor variability in vascular responses. Furthermore, increases in hypoxia at the tumor base could exacerbate fluence rate heterogeneities because the penetration of 630 nm light decreases under hypoxic conditions.[12,20]

A second observation stemming from these data is a potential effect of the tumor vascular microenvironment on the sensitivity of fluence rate response to PDT. This expectation stems from data that find actual fluence rates of 127 mW cm^{-2} in the tumor surface, 55 mW cm^{-2} in the tumor surface, and 37 mW cm^{-2} in the tumor base to produce similar hypoxic and cytotoxic effects, namely EF3 binding of ~20–30 units and a plating efficiency immediately after PDT of ~20%, while a fluence rate of 93 mW cm^{-2} in the tumor base produced over twice as much hypoxia (66 EF3 binding units) and protected from cell death (plating efficiency 30%). Thus, the tumor base appeared very sensitive to the difference between fluence rates of 37 and 93 mW cm^{-2}, but the tumor surface was insensitive to the difference between fluence rates of 127 and 55 mW cm^{-2}. Our studies suggest that, compared to their surfaces, the base of the tumors have more effective vasculature, characterized by more dense vascular spacing and better perfusion in the absence of any overall differences in the total vascular fraction in the tumor base *vs.* surface. Additionally, trends toward a greater fraction of smooth muscle actin, a marker of vessel maturity, in the tumor base further suggest that the tumor base may have greater potential to mount an acute vascular response to a stimulus such as PDT. Indeed, others have used models to demonstrate that heterogeneity in tumor vasculature affects adaptation of its bloods vessels to hemodynamic stimuli.[21] Moreover, acute, but reversible, vascular spasm during PDT has been previously reported,[18,22] which could lead to the creation of transient hypoxia during PDT that protects tumor and endothelial cells.

Intratumoral regional differences in vascular development are not unique to only this tumor model. Human malignant melanomas demonstrate higher vascularity at the tumor base compared to their centers,[23] and in ocular (uveal) melanomas the tumor base exhibits a higher prevalence of smooth muscle actin-stained vessels compared to other tumor regions.[24] Patterns in vascular development have also been noted in ovarian cancer; in a study that utilized power Doppler ultrasound the majority of malignant lesions of ovarian carcinoma demonstrated vascularization that extended into the tumor from one distinct edge with the normal tissue.[25] Thus, given the extent of knowledge on the presence of significant heterogeneity in tumor vascular networks,[26,27] it seems relevant to perform these studies in a model in which intratumor heterogeneity in vascular structure exists. However, that said, it is also important that the orientation of any differentials in vascular development relative to differentials in light distribution during PDT will not confound interpretation of the data. In the present study this is accomplished because the tumor region exhibiting the most PDT-sensitive vasculature (*i.e.* the base) was also the most distant from the light source and thus received a lower total light dose than its surface. In other words, increased responsiveness at the base was seen not due to the delivery of a higher fluence, but in spite of a lower fluence. Nevertheless, in other tumors, heterogeneity in vascular development could be oriented differently relative to light distribution, which could impact upon the presence and extent of fluence rate effects. Ultimately, *in vivo* monitoring of tumor hemodynamic parameters during PDT could provide a means of assessing the potential benefit of fluence rate manipulation in a given tumor.[28]

A key conclusion from this study is that low fluence rate significantly reduced depth-dependent regional heterogeneity in hypoxia during PDT. This necessitated that low fluence rate overcome the effects of depth-dependent gradients in light distribution, as well as any sensitivity of the tumor base to PDT. Ultimately, the lower fluence rate reduced heterogeneity in vascular response during PDT, and the hypoxia and clonogenicity data indicate that this was through its more mild effect on the tumor base. It has previously been shown that the advantages of low fluence rate include preservation of tumor oxygenation during PDT,[29,30] as well as reduction in gradients in hypoxia as a function of distance from a blood vessel.[4,31] This is consistent with the current data that show PDT at 38 mW cm^{-2} to produce less hypoxia in the tumor base than treatment at the higher fluence rate of 75 mW cm^{-2} (actual fluence rate in the base measured as 37 mW cm^{-2} *vs.* 93 mW cm^{-2}, respectively).

Vascular response to 38 mW cm^{-2} was not only more spatially homogeneous, but also more temporally homogeneous, namely it returned to and remained around pre-illumination levels during the latter part of the treatment. These data suggest that the additional illumination time at low fluence rate may provide an independent treatment advantage, as has been recently reported in other studies.[32] Furthermore, given the finding that the fluence used in this study appeared to be close to the minimum threshold required for a curative response (2/14 cures), the return of blood flow to pre-treatment levels during the end of 38 mW cm^{-2} PDT suggests that longer treatments (high fluences) could increase the differential in tumor response between 38 mW cm^{-2} and 75 mW cm^{-2} PDT.

The data from this study indicate that significant hypoxia was created during PDT, despite findings that treatment initially triggered an increase in blood flow. These results are easily reconciled by the facts that blood flow increases were transient and the hypoxia marker assay reports on hypoxia created throughout PDT, with the data weighted as a function of the severity and duration of this hypoxia.[33] In other words, it is possible

for severe hypoxia for short times to result in substantial EF3 binding. The DCS data suggest that periods of perfusion-related severe hypoxia are indeed likely because in tumors treated at 75 mW cm^{-2} PDT normalized blood flow was less than 0.5 for ~20% of the treatment. Furthermore, it is also plausible that any increases in oxygen delivery secondary to PDT-triggered increases in blood flow are insufficient to offset initial, rapid decreases in tumor oxygenation, which result from photochemical oxygen consumption and have been found at low fluences during even low fluence rate treatments.[18]

Another interesting observation stemming from this study is the presence of fluctuations in blood flow in a subset of the animals exposed only to control conditions, including no photosensitizer (light alone) and no photosensitizer or light. These fluctuations were curiously not present in every animal. Importantly, they were also significantly smaller than changes in blood flow induced by PDT, thus they did not interfere with data interpretation in the context of this study. Nevertheless, it is scientifically valuable to consider their cause, and our investigation of this phenomena indicates that individual mice can respond differently to anesthesia (isoflurane) with some exhibiting a steady heart rate and breathing rate throughout the duration of anesthesia, while others demonstrate fluctuations in heart rate and breathing rate. Not surprisingly, such fluctuations can also lead to variability in tumor blood flow (data not shown).

In summary, the data of the present report document the presence of and demonstrate the biological relevance of depth-dependent regional differences in vascular and cytotoxic responses during PDT. The tumor base appeared to be more sensitive to the effects of PDT than the tumor surface, and differentials in PDT response between the regions were likely contributed to by differences in the vasculature network of the tumor base compared to its surface. Importantly, these heterogeneities were overcome by lowering the PDT fluence rate, with the data showing that low fluence rate allowed for greater homogeneity in vascular, hypoxic, and cytotoxic responses. Overall, these data support the conclusion that the benefits of low fluence rate PDT are mediated in part through its ability to produce more homogenous PDT responses at both a microscopic[4] and macroscopic (present report) level.

Abbreviations

DCS	Diffuse correlation spectroscopy
EF3	[(2-(2-Nitroimidazol-1*H*-yl)-*N*-(3,3,3-trifluoropropyl)acetamide)
HPPH	2-(1-Hexyloxyethyl)-2-devinyl pyropheophorbide-a
PDT	Photodynamic therapy
THC	Total hemoglobin concentration

Acknowledgements

We gratefully acknowledge Elizabeth Rickter, Min Yuan, and Shirron Carter, Department of Radiation Oncology, for technical support. We acknowledge Drs H. Mark Saunders and Chandra Sehgal for assistance with power Doppler ultrasound, Dr Cameron Koch for his contribution to studies utilizing EF3, and Dr Jarod Finlay for useful discussions on this work. These studies were supported by NIH grants CA085831 and CA87971.

References

1 S. Coutier, L. N. Bezdetnaya, T. H. Foster, R. M. Parache and F. Guillemin, Effect of irradiation fluence rate on the efficacy of photodynamic therapy and tumor oxygenation in meta-tetra (hydroxyphenyl) chlorin (mTHPC)-sensitized HT29 xenografts in nude mice, *Radiat. Res.*, 2002, **158**, 339–345.
2 T. M. Sitnik and B. W. Henderson, The effect of fluence rate on tumor and normal tissue responses to photodynamic therapy, *Photochem. Photobiol.*, 1998, **67**, 462–466.
3 E. Angell-Petersen, S. Spetalen, S. J. Madsen, C. H. Sun, Q. Peng, S. W. Carper, M. Sioud and H. Hirschberg, Influence of light fluence rate on the effects of photodynamic therapy in an orthotopic rat glioma model, *J. Neurosurg.*, 2006, **104**, 109–117.
4 T. M. Busch, E. P. Wileyto, M. J. Emanuele, F. Del Piero, L. Marconato, E. Glatstein and C. J. Koch, Photodynamic therapy creates fluence rate-dependent gradients in the intratumoral spatial distribution of oxygen, *Cancer Res.*, 2002, **62**, 7273–7279.
5 B. W. Henderson, T. M. Busch and J. W. Snyder, Fluence rate as a modulator of PDT mechanisms, *Lasers Surg. Med.*, 2006, **38**, 489–493.
6 S. Iinuma, K. T. Schomacker, G. Wagnieres, M. Rajadhyaksha, M. Bamberg, T. Momma and T. Hasan, In vivo fluence rate and fractionation effects on tumor response and photobleaching: photodynamic therapy with two photosensitizers in an orthotopic rat tumor model, *Cancer Res.*, 1999, **59**, 6164–6170.
7 M. B. Ericson, C. Sandberg, B. Stenquist, F. Gudmundson, M. Karlsson, A. M. Ros, A. Rosen, O. Larko, A. M. Wennberg and I. Rosdahl, Photodynamic therapy of actinic keratosis at varying fluence rates: assessment of photobleaching, pain and primary clinical outcome, *Br. J. Dermatol.*, 2004, **151**, 1204–1212.
8 B. W. Henderson, S. O. Gollnick, J. W. Snyder, T. M. Busch, P. C. Kousis, R. T. Cheney and J. Morgan, Choice of oxygen-conserving treatment regimen determines the inflammatory response and outcome of photodynamic therapy of tumors, *Cancer Res.*, 2004, **64**, 2120–2126.
9 K. K. Wang, S. Mitra and T. H. Foster, A comprehensive mathematical model of microscopic dose deposition in photodynamic therapy, *Med. Phys.*, 2007, **34**, 282–293.
10 H. W. Wang, T. C. Zhu, M. E. Putt, M. Solonenko, J. Metz, A. Dimofte, J. Miles, D. L. Fraker, E. Glatstein, S. M. Hahn and A. G. Yodh, Broadband reflectance measurements of light penetration, blood oxygenation, hemoglobin concentration, and drug concentration in human intraperitoneal tissues before and after photodynamic therapy, *J. Biomed. Opt.*, 2005, **10**, 14004.
11 C. Holmer, K. S. Lehmann, J. Wanken, C. Reissfelder, A. Roggan, G. Mueller, H. J. Buhr and J. P. Ritz, Optical properties of adenocarcinoma and squamous cell carcinoma of the gastroesophageal junction, *J. Biomed. Opt.*, 2007, **12**, 014025.
12 S. Mitra and T. H. Foster, Carbogen breathing significantly enhances the penetration of red light in murine tumours in vivo, *Phys. Med. Biol.*, 2004, **49**, 1891–1904.
13 T. M. Busch, E. P. Wileyto, S. M. Evans and C. J. Koch, Quantitative spatial analysis of hypoxia and vascular perfusion in tumor sections, *Adv. Exp. Med. Biol.*, 2003, **510**, 37–43.
14 H.-W. Wang, E. Rickter, M. Yuan, E. P. Wileyto, E. Glatstein, A. Yodh and T. M. Busch, Effect of photosensitizer dose on fluence rate responses to photodynamic therapy, *Photochem. Photobiol.*, 2007, **83**, 1040–1048.
15 H. W. Wang, M. E. Putt, M. J. Emanuele, D. B. Shin, E. Glatstein, A. G. Yodh and T. M. Busch, Treatment-induced changes in tumor oxygenation predict photodynamic therapy outcome, *Cancer Res.*, 2004, **64**, 7553–7561.
16 G. Yu, T. Durduran, C. Zhou, H. W. Wang, M. E. Putt, H. M. Saunders, C. M. Sehgal, E. Glatstein, A. G. Yodh and T. M. Busch, Noninvasive monitoring of murine tumor blood flow during and after photodynamic therapy provides early assessment of therapeutic efficacy, *Clin. Cancer Res.*, 2005, **11**, 3543–3552.
17 T. M. Busch, S. M. Hahn, E. P. Wileyto, C. J. Koch, D. L. Fraker, P. Zhang, M. Putt, K. Gleason, D. B. Shin, M. J. Emanuele, K. Jenkins, E. Glatstein and S. M. Evans, Hypoxia and Photofrin uptake in the intraperitoneal carcinomatosis and sarcomatosis of photodynamic therapy patients, *Clin. Cancer Res.*, 2004, **10**, 4630–4638.
18 T. M. Sitnik, J. A. Hampton and B. W. Henderson, Reduction of tumour oxygenation during and after photodynamic therapy in vivo: effects of fluence rate, *Br. J. Cancer*, 1998, **77**, 1386–1394.

19 M. Seshadri, J. A. Spernyak, R. Mazurchuk, S. H. Camacho, A. R. Oseroff, R. T. Cheney and D. A. Bellnier, Tumor vascular response to photodynamic therapy and the antivascular agent 5,6-dimethylxanthenone-4-acetic acid: implications for combination therapy, *Clin. Cancer Res.*, 2005, **11**, 4241–4250.
20 K. P. Nielsen, A. Juzeniene, P. Juzenas, K. Stamnes, J. J. Stamnes and J. Moan, Choice of optimal wavelength for PDT: the significance of oxygen depletion, *Photochem. Photobiol.*, 2005, **81**, 1190–1194.
21 A. R. Pries, A. J. Cornelissen, A. A. Sloot, M. Hinkeldey, M. R. Dreher, M. Hopfner, M. W. Dewhirst and T. W. Secomb, Structural adaptation and heterogeneity of normal and tumor microvascular networks, *PLoS Comput. Biol.*, 2009, **5**, e1000394.
22 B. Chen, B. W. Pogue, P. J. Hoopes and T. Hasan, Combining vascular and cellular targeting regimens enhances the efficacy of photodynamic therapy, *Int. J. Radiat. Oncol., Biol., Phys.*, 2005, **61**, 1216–1226.
23 B. Dome, S. Paku, B. Somlai and J. Timar, Vascularization of cutaneous melanoma involves vessel co-option and has clinical significance, *J. Pathol.*, 2002, **197**, 355–362.
24 Y. Pina, C. M. Cebulla, T. G. Murray, A. Alegret, S. R. Dubovy, H. Boutrid, W. Feuer, L. Mutapcic and M. E. Jockovich, Blood vessel maturation in human uveal melanoma: spatial distribution of neovessels and mature vasculature, *Ophthalmic Res.*, 2009, **41**, 160–169.
25 S. Kupesic and A. Kurjak, Contrast-enhanced, three-dimensional power Doppler sonography for differentiation of adnexal masses, *Obstet. Gynecol.*, 2000, **96**, 452–458.
26 J. A. Nagy, S. H. Chang, A. M. Dvorak and H. F. Dvorak, Why are tumour blood vessels abnormal and why is it important to know?, *Br. J. Cancer*, 2009, **100**, 865–869.
27 D. Fukumura and R. K. Jain, Tumor microvasculature and microenvironment: targets for anti-angiogenesis and normalization, *Microvasc. Res.*, 2007, **74**, 72–84.
28 J. H. Woodhams, A. J. Macrobert and S. G. Bown, The role of oxygen monitoring during photodynamic therapy and its potential for treatment dosimetry, *Photochem. Photobiol. Sci.*, 2007, **6**, 1246–1256.
29 T. M. Busch, Local physiological changes during photodynamic therapy, *Lasers Surg. Med.*, 2006, **38**, 494–499.
30 W. J. Cottrell, A. D. Paquette, K. R. Keymel, T. H. Foster and A. R. Oseroff, Irradiance-dependent photobleaching and pain in delta-aminolevulinic acid-photodynamic therapy of superficial basal cell carcinomas, *Clin. Cancer Res.*, 2008, **14**, 4475–4483.
31 T. H. Foster, R. S. Murant, R. G. Bryant, R. S. Knox, S. L. Gibson and R. Hilf, Oxygen consumption and diffusion effects in photodynamic therapy, *Radiat. Res.*, 1991, **126**, 296–303.
32 M. Seshadri, D. A. Bellnier, L. A. Vaughan, J. A. Spernyak, R. Mazurchuk, T. H. Foster and B. W. Henderson, Light delivery over extended time periods enhances the effectiveness of photodynamic therapy, *Clin. Cancer Res.*, 2008, **14**, 2796–2805.
33 T. M. Busch, S. M. Hahn, S. M. Evans and C. J. Koch, Depletion of tumor oxygenation during photodynamic therapy: detection by the hypoxia marker EF3 [2-(2-nitroimidazol-1[*H*]-yl)-*N*-(3,3,3,-trifluoropropyl)acetamide], *Cancer Res.*, 2000, **60**, 2636–2642.